Contribution from the Department of Chemistry,
Texas A&M University, College Station, Texas 77843

Ab Initio Molecular Orbital Calculations on Square-Pyramidal Iron Nitrosyls. Geometry and Electronic Structure of {FeNO}^{6}, {FeNO}^{7}, and {FeNO}^{8} Systems

T. W. HAWKINS and M. B. HALL*

Received July 25, 1979

Ab Initio molecular orbital calculations at several Fe–N–O bond angles are reported for $[Fe(CN)_4NO]^{n-}$ (n = 1–3) and for $[Fe(CO)_2(CN)_2NO]^-$. An important energetic contribution to the linear geometry of the {FeNO}^{6} species arises from interaction of the filled nitrosyl 5σ and 1π orbitals with the metal in addition to the interaction of the nitrosyl 2π orbital. The potential energy curve for the {FeNO}^{7} system is nearly flat in agreement with the wide variety of experimental geometries and with a poorly defined oxygen position in many X-ray structures for {MNO}^{7} systems. The ground state of this ion, $[Fe(CN)_4NO]^{2-}$, is predicted to be a linear $^2A_1$ state with considerable unpaired density in a $3d_{z^2}$ orbital in agreement with the X-ray structure, Mössbauer, and EPR data. The {FeNO}^{8} species show the expected bent geometry. The tendency for the nitrosyl to bend in the plane of the better π acceptor (CO plane in $[Fe(CO)_2(CN)_2NO]^-$) is confirmed, and a simple electrostatic rationale for this behavior is presented.

Introduction

Traditionally, linear metal nitrosyls have been classified as coordinated NO^+ while bent ones have been classified as coordinated NO^-.[1] Following this classification it was common to correlate the geometry with the nitrosyl stretching frequency (ν_{NO}).[2] However, recent work in both infrared and X-ray photoelectron spectroscopy indicated that this NO^+/NO^- classification was inadequate.[3] To alleviate this problem, Enemark and Feltham[4] introduced a notation in which the oxidation states of the metal and nitrosyl are grouped together as {MNO}^{n}, where n is the number of d electrons plus the number of nitrosyl electrons in excess of those on NO^+. In their classification {MNO}^{6} systems will have a nearly linear geometry, while {MNO}^{8} systems will be strongly bent. Several molecular orbital studies, utilizing extended Hückel (EH) methods[5,6] (both iterative and noniterative), support this classification and its correlation with the M–N–O angle.

The most extensive studies, other than that of Enemark and Feltham,[4] are those of Hoffmann and co-workers.[6] Although these studies are in general agreement with that of Enemark and Feltham, there are some important differences. A simplified MO diagram showing the interaction of a ML_4 fragment and the NO ligand is shown in Figure 1. An {MNO}^{6} system is filled through the d_{xy} orbital. For a {MNO}^{7} system the additional electron could be in either the (d_{z^2}–σ_{NO}) or the ($\pi^*_{x,y}$–$d_{xz,yz}$) which would result in a $^2A_1$ or ^2E state, respectively. Following Enemark and Feltham, the $^2A_1$ state would remain linear while the ^2E state would bend due to a first-order Jahn–Teller effect. However, the $^2A_1$ could be subject to second-order Jahn–Teller distortion and in the model of Hoffmann a distortion will result regardless of which orbital is occupied in the linear configuration. Experimentally, square-pyramidal {FeNO}^{7} systems display angles which range from 177° in $[Fe(CN)_4NO]^{2-}$[7] to 127° in FeNO(salen)[8] (salen = *N*,*N*-ethylenebis(salicylideniminato)). A related question is that of a barrier to bending which might arise if the (d_{z^2}–σ) orbital is filled first.[4,6]

In five-coordinate {MNO}^{8} complexes EH calculations suggest that the nitrosyl will bend in the plane of the stronger π acceptor. However, work on $Co(NO)Cl_2(P(CH_3)(C_6H_5)_2)_2$ indicates bending of the nitrosyl counter to this direction.[9] In addition this concept sheds little light on the bending plane of systems such as Fe(NO)(salen).[8] In an attempt to further our understanding of these problems, we report ab initio molecular orbital calculations on $[Fe(CN)_4NO]^{n-}$ (n = 1–3), which correspond to {FeNO}^{6}, {FeNO}^{7}, and {FeNO}^{8} systems, respectively, at four Fe–N–O angles. We have also studied the bending in both the cyanide and carbonyl plane of the {FeNO}^{8} model system $[Fe(CN)_2(CO)_2]^-$.

Table I. Bond Distances and Angles[a]

	Bond Distances (Å)		
Fe–N(1)	1.565	Fe–C(2)	1.892
N(1)–O	1.161	C(2)–N(3)	1.159
	Angles (Deg)		
C(2)–Fe–C(4)	87.3	Fe–C(2)–N(3)	180.0
N(1)–Fe–C(2)	102.5		

[a] See illustration 1.

Theoretical Section

The ab initio calculations reported in this work were performed on an Amdahl 470 V/6 computer (Texas A&M University Data Processing Center) using the ATMOL2 system of programs.[10] The calculations for the closed-shell species {FeNO}^{6} and {FeNO}^{8} were of the restricted Hartree–Fock–Roothaan (RHF) type,[11] while that for the open-shell {FeNO}^{7} system was of the unrestricted Hartree–Fock (UHF) type.[12]

(1) (a) Sidgewick, N. V.; Bailey, R. W. *Proc. R. Soc. London, Ser. A* **1934**, *144*, 521. (b) Moeller, T. *J. Chem. Educ.* **1946**, *23*, 441, 542. (c) Addison, C. C.; Lewis, J. *Q. Rev., Chem. Soc.* **1955**, *9*, 115. (d) Griffith, W. P.; Lewis, J.; Wilkinson, G. *J. Inorg. Nucl. Chem.* **1958**, *7*, 38. (e) Johnson, B. F. G.; McCleverty, J. A. *Prog. Inorg. Chem.* **1966**, *7*, 277. (f) Swinehart, J. H. *Coord. Chem. Rev.* **1967**, *2*, 385. (g) Griffith, W. P. *Adv. Organomet. Chem.* **1968**, *7*, 211. (h) Masek J. *Inorg. Chim. Acta, Rev.* **1969**, *3*, 99. (i) McGarrity, J. A. *MTP Int. Rev. Sci.: Phys. Chem., Ser. One* **1972**, *5*, 229. (j) Frenz, B. A.; Ibers, J. A *Ibid.* **1972**, *11*, 33. (k) Connely, N. G. *Inorg. Chim. Acta, Rev.* **1972**, *6*, 48.
(2) (a) Synder, D. A.; Weaver, D. L. *Inorg. Chem.* **1970**, *9*, 2760. (b) Pierpont, C. G.; Pucci, A.; Eisenberg, R. *J. Am. Chem. Soc.* **1971**, *93*, 3050. (c) Mingos, D. M. P.; Ibers, J. A. *Inorg. Chem.* **1971**, *10*, 1479. (d) Bottomley, F. *Acc. Chem. Res.* **1978**, *11*, 158.
(3) (a) Su, C. C.; Faller, J. W. *J. Organomet. Chem.* **1975**, *84*, 53. (b) King, F.; Leigh, G. J. *J. Chem. Soc., Dalton Trans.* **1977**, 429. (c) Holsboer, F.; Beck, W.; Bartunik, H. D. *Ibid.* **1972**, 1828.
(4) Enemark, J. H.; Feltham, R. D. *Coord. Chem. Rev.* **1974**, *13*, 339.
(5) (a) Rein, R.; Fukuda, N.; Win, H.; Clarke, G. A.; Harris, F. E. *J. Chem. Phys.* **1966**, *45*, 4743. (b) Pierpont, C. G.; Eisenberg, R. *J. Am. Chem. Soc.* **1971**, *93*, 4905. (c) Mingos, D. M. P. *Inorg. Chem.* **1973**, *12*, 1209.
(6) (a) Rossi, A. R.; Hoffmann, R. *Inorg. Chem.* **1974**, *13*, 365. (b) Hoffmann, R.; Chen, M.; Elian, M.; Rossi, A.; Mingos, D. M. P. *Ibid.* **1974**, *13*, 2666. (c) Hoffmann, R.; Chen, M. M-L.; Thorn, D. L. *Inorg. Chem.* **1976**, *16*, 503.
(7) (a) Schmidt, J.; Kuhi, H.; Dorn, W. L.; Kopf, J. *Inorg. Nucl. Chem. Lett.* **1974**, *10*, 55. (b) Kopf, J.; Schmidt, J. *Z. Naturforsch., B* **1977**, *32*, 275.
(8) Haller, K. J.; Johnson, P. L.; Feltham, R. D.; Enemark, J. H.; Ferrano, J. R.; Basile, L. J. *Inorg. Chim. Acta* **1979**, *33*, 119.
(9) Brock, C. P.; Collman, J. P.; Dolcetti, G.; Farnham, P. H.; Ibers, J. A.; Lester, J. E.; Reed, C. A. *Inorg. Chem.* **1973**, *12*, 1304.
(10) ATMOL2 system: Hillier, I. H.; Saunders, V. R., Chemistry Department, University of Manchester, Manchester, England.
(11) Roothaan, C. C. J. *Rev. Mod. Phys.* **1951**, *23*, 69.
(12) Pople, J. A.; Nesbet, R. K. *J. Chem. Phys.* **1954**, *22*, 571.

0020-1669/80/1319-1735$01.00/0

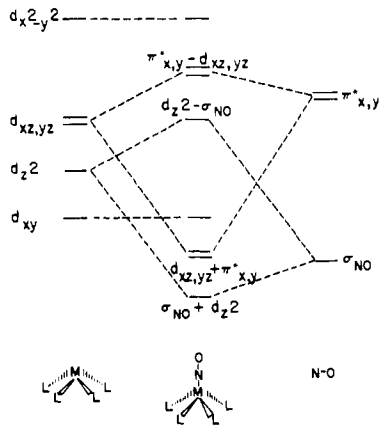

Figure 1. Schematic molecular orbital diagram for a five-coordinate square-pyramidal metal nitrosyl.

Table II. Simulated Ligand Results

property	actual CO	simulated CO[a]
	MO Energies (au)	
2π	+0.126	+0.124
5σ	−0.570	−0.567
1π	−0.665	−0.642
	MO Coefficients	
2π C 2p	0.973	1.013
5σ C 2s	0.795	0.826
C 2p	0.574	0.562

[a] CN basis with N nuclear charge of 7.8.

The geometry was based on the X-ray structure of $[Fe(CN)_4NO]^{2-}$.[7] The coordinate system is shown below (**1**) and the bond distances and

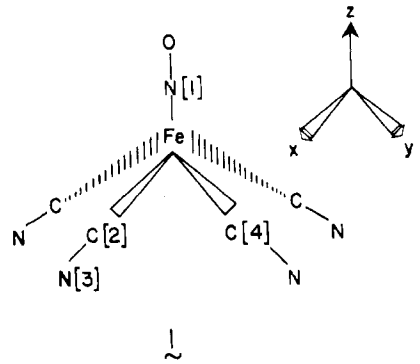

1

angles are given in Table I. Four Fe–N–O angles were chosen: 180, 155, 135, 105°. The bend is carried out in the *xz* plane, and the geometry of $Fe(CN)_4NO$ is fixed except for the Fe–N–O angle. Thus, we have not attempted to account for the observation that the M–N distances of bent $\{MNO\}^8$ molecules are longer than those of linear $\{MNO\}^6$ molecules.

All s and p orbitals of the iron and all s orbitals on the ligand atoms are best atom Slater type orbitals[13] expanded in three Gaussians.[14] The ligand 2p orbitals were represented by a three-Gaussian expansion of the atomic Hartree–Fock orbitals.[15] The iron 3d orbitals were the double-ζ Slater functions of Richardson et al.[16] for Fe(1+) expanded in four Gaussians. Following the suggestion of Hay,[17] we added an additional diffuse Gaussian to this basis to allow the iron d functions more flexibility. This latter basis is referred to as the 2D basis, while the former smaller basis is referred to as the 1D basis.

For the sake of economy, the CO ligands in the model complex $[Fe(CN)_2(CO)_2NO]^-$ were represented by a simulated ligand technique.[18] In this approach the basis functions and integrals are retained for the CN^- moiety while the nuclear charge on N is changed to make the CN^- ligand resemble CO. A comparison between an actual CO calculation and our simulated CO is shown in Table II. A cursory inspection of the results indicates that this approach reproduces the MO energies and coefficients with surprising accuracy.

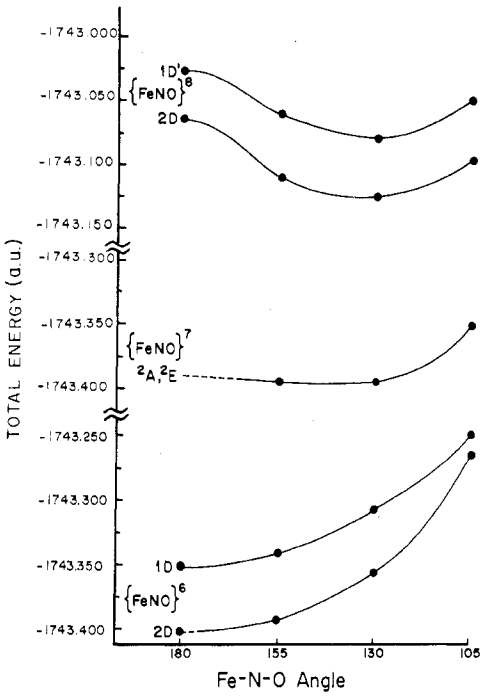

Figure 2. Potential energy curves for $[Fe(CN)_4NO]^{n-}$ (n = 1–3) which are examples of $\{FeNO\}^6$, $\{FeNO\}^7$, and $\{FeNO\}^8$ complexes, respectively. The 2D calculation has an additional 3d Fe basis function.

Results and Discussion

$[Fe(CN)_4NO]^-$. The potential energy curve for bending of this $\{FeNO\}^6$ species is shown at the bottom of Figure 2. As expected, the linear Fe–N–O geometry is the most stable. While the larger basis (2D) has a lower total energy and shows a somewhat deeper minimum, it is qualitatively similar to the smaller basis (1D).

A partial Walsh-type MO diagram for this system is shown in Figure 3. The two lowest energy unoccupied orbitals are $17a_1$ and the 12e. The $17a_1$ is mainly Fe $3d_{z^2}$ and Fe $4p_z$ hybridized away from the nitrosyl with some antibonding 5σ NO character. The 12e is an antibonding combination of NO $2\pi_{x,y}$ and Fe $3d_{xz,yz}$. The 12 highest occupied MO's are mainly 1π CN^- and N lone pair on CN^-. These orbitals are listed in Figure 3 (in the bent C_{2v} notation), but they are not drawn since they are insensitive to the Fe–N–O angle. In EH calculations, these orbitals are predicted to lie much lower in energy because of the neglect of the electron–electron repulsions. The highest occupied orbital that shows significant changes on bending is the 8e, which is composed primarily of Fe $3d_{xz,yz}$, NO $2\pi_{x,y}$ and CN^- 5σ. This orbital is Fe–NO π bonding and Fe–CN^- σ antibonding. The $4b_1$ orbital is bonding between the Fe $3d_{x^2-y^2}$ and the b_1 combination of CN^- σ orbitals. The $1b_2$ orbital is mainly Fe $3d_{xy}$, while the 7e is mainly Fe $3d_{xy,yz}$ bonding with the e combination of CN^- orbitals. The $14a_1$ MO can be identified as the a_1 combination of CN^- σ orbitals stabilized by interaction with the Fe $3d_{z^2}$, 4s, and $4p_z$. The 6e orbital is primarily NO 1π slightly stabilized by the Fe $3d_{xz,yz}$. The $13a_1$ is the NO 5σ stabilized by interaction with the metal, while the $12a_1$ is the NO 4σ.

(13) Clementi, E.; Raimondi, D. L. *J. Chem. Phys.* **1963**, *38*, 2686.
(14) Stewart, R. F. *J. Chem. Phys.* **1970**, *52*, 431.
(15) Stewart, R. F. *J. Chem. Phys.* **1969**, *50*, 2485.
(16) Richardson, J. W.; Nieuwpoort, W. C.; Powell, R. R.; Edgell, W. F. *J. Chem. Phys.* **1962**, *36*, 1057.
(17) Hay, P. J. *J. Chem. Phys.* **1977**, *66*, 4377.
(18) Hawkins, T. W. M.S. Thesis, Texas A&M University, May 1979.
(19) Mulliken, R. S. *J. Chem. Phys.* **1955**, *23*, 1841.

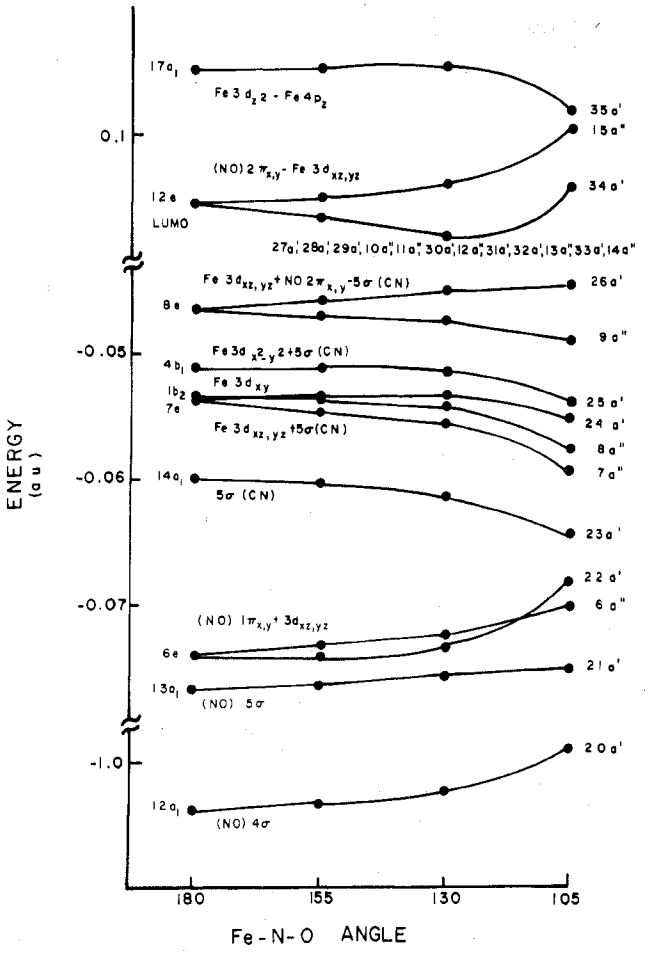

Figure 3. Walsh-type molecular orbital diagram for the {FeNO}^{6} complex, $[Fe(CN)_4NO]^-$.

As the nitrosyl bends, the orbital which shows the greatest rise in energy is the 6e. This orbital is primarily 1π nitrosyl which on bending splits into an a′ and a″ (C_s). The a′ component now interacts with the NO 5σ, which is being destablized by loss of the bonding to the metal, resulting in a net destabilization. This destabilization is due to a filled-orbital, filled-orbital interaction much like the close approach of two inert gas atoms. Previous semiempirical calculations[4-6] have emphasized the loss of the nitrosyls' π-acceptor ability and the destabilization of the metal $3d_{xz}$ orbital (bending in xz plane). Figure 3 also shows this behavior in the splitting of the 8e into 9a″ and 26a′, with the 26a′ being destabilized. However, the ab initio results suggest that this is less important than the filled orbital replusion in the 6e and $13a_1$.

The approximate charge distribution (Mulliken population analysis) is shown in the left-hand side of Figure 4. The NO ligand is essentially neutral, the Fe is close to +1, while each CN ligand has a −0.5 charge. There is very little charge redistribution during bending, except for a rearrangement of charge between the Fe $3d_{z^2}$ and $3d_{xz}$ and between the N and O $2p_x$ and $2p_y$ orbitals. As the nitrosyl bends, the Fe $3d_{z^2}$ gains electron density at the expense of the Fe $3d_{xz}$ orbital. This occurs in the bent geometry because the $3d_{z^2}$ is being stabilized by the 2π nitrosyl orbital while the $3d_{xz}$ is being destabilized by the 5σ nitrosyl.

$[Fe(CN)_4NO]^{2-}$. In forming this {FeNO}^{7} species from the linear {FeNO}^{6} species the additional electron could be placed in either the 12e or $17a_1$ leading to a ^2E or $^2A_1$ state, respectively. Although the $17a_1$ MO is higher in energy than the 12e MO in the {FeNO}^{6} species, the UHF calculation predicts the $^2A_1$ state to be slightly lower in energy than the

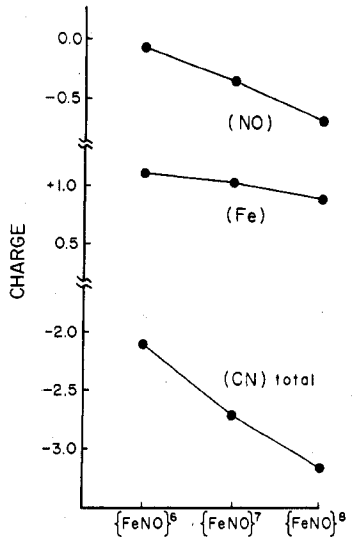

Figure 4. Mulliken-type charge distribution for the {FeNO}^{6}, {FeNO}^{7}, and {FeNO}^{8} tetracyanonitrosyliron complexes.

^2E state. A spin density analysis of the $^2A_1$ state shows that 81% of the majority spin density resided in the $3d_{z^2}$ orbital of iron.[20] These results are in agreement with the Mössbauer[21] and EPR spectra[7a,22] and with a simplified MO calculation by Dorn and Schmidt.[22] The value of S^2 for this state is large (1.8) due to the tendency of UHF calculations to mix in states of higher multiplicity ($S = {}^3/_2$). The degree of mixing is quite large in this case suggesting a close-lying excited quartet state. Experimentally one finds doublet and quartet states very close in Fe(NO)(salen)[8] and Fe(NO)(TMC)$^{2+}$ (TMC = 1,4,8,11-tetramethyl-1,4,8,11-tetraazacyclotetradecane).[23] This spin polarization also causes significant amounts of spin density to reside on the ligands. Although the calculations probably overestimate the polarization, because of the mixing in of the $S = {}^3/_2$ state, our result lends support to the idea[22] that spin polarization is responsible for the observed hyperfine coupling (10 G) with ^{13}C of the equatorial cyanides.

The potential energy curve for the {FeNO}^{7} system is shown in the middle of Figure 2 (1D basis). We have not shown the positions of the ^2E and $^2A_1$ at 180° because we feel that they are too close in energy for calculations at this level to yield more than a qualitative description.[24] The ^2E state would be Jahn–Teller unstable and the calculation predicts that this state would bend with a minimum energy near 135°. However the curve is extremely flat; the difference in energy between 180 and 130° is less than 3 kcal/mol. In the bent geometry the ground state is a $^2A'$ state with the $^2A''$ state lying higher in energy. The linear $^2A_1$ state, which is predicted to be the ground state, could distort through a second-order Jahn–Teller effect (mixing with the ^2E, since in the C_s geometry one component of the ^2E is of $^2A'$ symmetry, as is the $^2A_1$). Our result indicates that the $^2A_1$ energy is slightly below the energy of the 135° geometry suggesting a small barrier to bending. These results must be taken with a note of caution because

(20) Although the unrestricted nature of the calculations precludes our actually calculating the g values, we can make some qualitative observations about these values from the orbital character. The linear $^2A_1$ state would have $g_z = g_e$ and $g_x = g_y > g_e$ in agreement with experiment. Although, bending the Fe–N–O system as much as 25° will not change significantly the g values, occupying one of the e orbitals instead of the a_1 would produce a significant change in their values in disagreement with experiment.

(21) Raynor, J. B. *J. Inorg. Nucl. Chem.* **1970**, *33*, 735.
(22) Dorn, W. L.; Schmidt, J. *Inorg. Chim. Acta* **1976**, *16*, 223.
(23) Hodges, K. D.; Wollman, R. G.; Kessel, S. L.; Hendrickson, D. N.; Van Derveer, D. G.; Barefield, E. K. *J. Am. Chem. Soc.* **1979**, *101*, 906

(24) This is due in part to the differing amount of spin contamination in these two states.

of the small basis and the lack of configuration interaction. However, the qualitative result that {FeNO}^{7} systems have a very flat potential energy curve with respect to bending should prevail. This result is consistent with recent IR work[25] and with the poor definition of the Fe–N–O geometry, because of large thermal motion of the oxygen in the structural characterization of $Fe(NO)[S_2CN(C_2H_5)_2]_2$,[26] $Fe(NO)[S_2CN(C_3H_3)_2]_2$,[27] $Fe(NO)[S_2C_2(CN)_2]_2^{2-}$,[28] and $[Fe(CN)_4NO]^{2-}$.[7b] The results also suggest that the geometries and electronic states may be influenced by environmental factors such as solvent effects and crystal packing as well as by small changes in the other ligands. Examples of the latter include the work of Enemark and Feltham on the stereochemical control of valence in {FeNO}^{7} systems.[29] For the characterization of the relative energies of various states and their behavior under Fe–N–O angle deformations, calculations in larger basis sets, with configuration interaction, and at more points along the potential curve will be necessary.

Although the additional electron added to form $[Fe(CN)_4NO]^{2-}$ from $[Fe(CN)_4NO]^-$ enters an orbital which is primarily iron and nitrosyl, the final self-consistent charges (Figure 4) show very little change in the iron charge, less than half of the additional electron remains on the nitrosyl, and more than half ends up on the cyanides. Thus, the cyanides act as an electron sink and the iron is simply transmitting these electrons. This type of rearrangement of charge is not seen in the non-self-consistent EH calculations.

$[Fe(CN)_4NO]^{3-}$. The potential energy curves for the {FeNO}^{8} species show a minimum for a strongly bent geometry (Figure 2). Although there are no structural data available for this complex, the nitrosyl stretching frequency of 1555 cm^{-1} [30] is consistent with a bent structure. The predicted angle of ~130° is also consistent with a variety of known {MNO}^{8} systems. The energy of the split d orbital basis (2D) is lower for all geometries but is in qualitative agreement with the smaller basis (1D).

The results show a significant barrier to forcing the Fe–N–O system to be linear. However, this barrier is probably overestimated by the RHF calculations because the lowest energy linear configuration $12e^2$ is a mixture of the $^1A_1$ and $^1B_1$ states in this approximation. It might be better to view this 180° calculation as the correct single determinant of a nearly linear Fe–N–O, since in the C_s point group the $^1A'$ state is a mixture of $^1A_1$ and $^1B_1$. Although the lowest energy configuration of the {FeNO}^{7} system has one electron in the $17a_1$, placing two electrons in this orbital leads to a $^1A_1$ state which is 0.5 eV above the energy of the $12e^2$ configuration.

As the system bends, the $17a_1$ and 12e orbitals mix as shown in Figure 5, where the HOMO contains both Fe $3d_{z^2}$ and $3d_{xz}$ as well as NO $2\pi_x$. Furthermore, the HOMO is the only orbital which shows significant stabilization on bending. The remaining orbitals are either slightly destabilized or unchanged (not shown on the diagram but their symmetry characters are listed at their appropriate positions). The orbitals at 180° are still in the C_s point group, so one should view this result as the best single determinant for a nearly linear system. The domination of the geometry by the HOMO in {FeNO}^{8} systems is consistent with the previous approximate MO descriptions.

As in the previous reduction from {FeNO}^{6} to {FeNO}^{7}, the additional electron added to {FeNO}^{8} causes substantial rearrangement of the charge density. The cyanide ligands gain nearly 0.45 electron, the nitrosyl gains about 0.40 electron, and the iron gains 0.15 electron. The overall change in going from {FeNO}^{6} to {FeNO}^{8} results in a gain of one electron by the four cyanides, a gain of three-fourths of an electron by the nitrosyl, and a gain of one-fourth of an electron by the iron. Thus, in the two-electron reduction of a formally NO^+ complex to a formally NO^- complex, less than one electron actually remains on the NO. However, in the bent {FeNO}^{8} system the NO ligand bears an overall negative charge (see Figure 4) and would be nucleophilic. The remaining electron density is divided equally between the iron and each of the four cyanides. Approximately 90% of the electron gain in the cyanides is in the σ system with less than a 10% change in the π electron density. Since the 5σ cyanide orbital is antibonding between C and N, this increase should decrease the CN stretching frequency.[31] Although the cyanide stretching frequency for the {FeNO}^{6} species is not available, the {FeNO}^{7} species, $[P(C_6H_5)_4]_2[Fe(CN)_4NO]$, has a ν_{CN} of 2110 cm^{-1}, while the {FeNO}^{8} species, $K_3[Fe(CN)_4NO]$, has a ν_{CN} of 2045 cm^{-1}.[30] The importance of the 5σ orbital occupation in determining the cyanide stretching frequency has also been emphasized by Fenske and DeKock.[31]

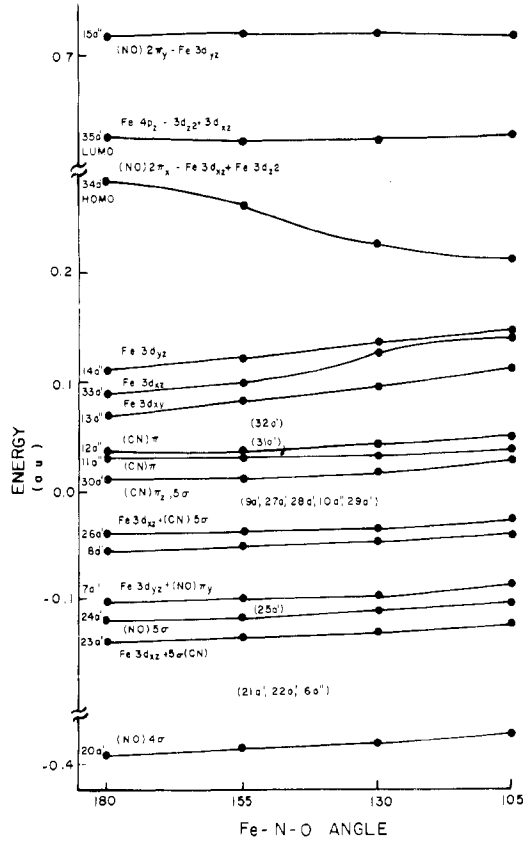

Figure 5. Walsh-type molecular orbital diagram for the {FeNO}^{8} complex, $[Fe(CN)_4NO]^{3-}$. The point group is C_s, so that the points at "180" should be viewed as the results of the best single determinant for a nearly linear Fe–N–O system (see text).

$[Fe(CO)_2(CN)_2NO]^-$. We have used the previously mentioned ligand simulation technique to calculate the potential energy curves of this {FeNO}^{8} complex. The potential energy curve for bending the nitrosyl in the trans cyanide plane (NC–Fe–CN) is compared to that for bending in the trans carbonyl plane (OC–Fe–CO) in Figure 6. Since this is an {FeNO}^{8} complex, one expects a bent structure to be favored in either plane. The potential energy curve for the bend in

(25) Quinby-Hunt, M.; Feltham, R. D. *Inorg. Chem.* **1978**, *17*, 2515.
(26) Colapietro, J.; Domenicano, A.; Scaramuzza, L.; Vaciago, A.; Zambonelli, L. *Chem. Comm.* **1967**, 583.
(27) Davies, G. R.; Mais, R. H. B.; and Owston, P. G. *Chem. Comm.* **1968**, 81.
(28) Rae, I. M. *Chem. Commun.* **1967**, 1245.
(29) Enemark, J. H.; Feltham, R. D.; Huie, B. T.; Johnson, P. L.; Swedo, K. B. *J. Am. Chem. Soc.* **1977**, *99*, 3285.
(30) Nast, V. R.; Schmidt, J. *Z. Anorg. Allg. Chem.* **1976**, *421*, 15.
(31) Fenske, R. F.; DeKock, R. L. *Inorg. Chem.* **1972**, *11*, 437.

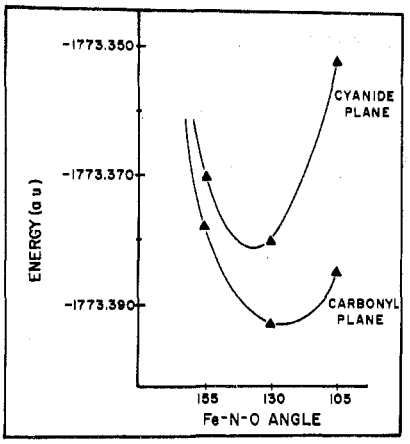

Figure 6. Potential energy curves for $[Fe(CO)_2(CN)_2NO]^-$ with the nitrosyl bent in the plane of the cyanide ligands and in the plane of the carbonyl ligands.

the cyanide plane shows a minimum at 136°, while that for the carbonyl plane shows a minimum at 126°. Thus, not only does the system have a lower total energy when bent in the carbonyl plane but it assumes a more strongly bent geometry.

The $Co(NO)Cl_2(PR_3)_3$ complexes show two IR stretching frequencies attributable to two different nitrosyl structures. Brock et al.[9] believe the complexes to be a mixture of trigonal-bipyramidal and square-pyramidal $Co(NO)Cl_2(PR_3)_2$ in equilibrium. However, the possibility of two distinct conformers in which the nitrosyl is simply bent in two different planes has been suggested by Enemark and Feltham[4] as an alternative explanation of the unusual IR results. Although our results provide no direct evidence on this question, the relatively small energy difference (7 kcal/mol) between the two bent conformers of $[Fe(CO)_2(CN)_2(NO)]^-$ suggests that an equilibrium mixture of two $Co(NO)Cl_2(PR_3)_2$ conformers could exist if their energy difference was small enough.

In order to gain insight into the preferential bending in the carbonyl plane, we compared the behavior of the MO's for the deformation in the two planes. This Walsh type of analysis was unable to identify any one or any group of orbitals which could be rationalized as stabilizing one conformer over the other. Likewise, a simple comparison of orbital energies between the two structures at an Fe–N–O angle of 130° (closest to the equilibrium geometry of both conformers) revealed little change. We have, therefore, attempted to analyze the total energy in a more direct manner. A note of caution must be made; since any partitioning of the large number of terms in the total energy is arbitrary, different schemes may arrive at what appear to be different explanations of the preferred geometry. Also, the results may depend on the basis set chosen and on the use of only a single determinant wave function. With these difficulties in mind, we have partitioned the total energy (TE) into the simplest physical division of kinetic (KE) and potential energy (PE). We then further divided the PE into nuclear repulsion (NR), nuclear–electron attraction (NA), and electron–electron repulsion (ER). Thus

$$TE = KE + NR + NA + ER$$

An analysis of these energy contributions to the two conformers at an Fe–N–O angle of 130° is shown in Table III. The bend in the CN plane is favored by three of the four energy terms, while the bend in the CO plane is only favored by the nuclear–electron attraction (NA) term. The NA term is sufficiently large to cause the 130° CO plane to be the conformer of lower total energy.

Table III. Total Energy Partitioning for $Fe[(CO)_2(CN)_2]^-$ at a 130° Fe–N–O Angle[a]

contributions	CO plane	CN plane	differences
kinetic energy	+1733.546	+1733.502	−0.044
nuclear repulsns	+792.532	+792.480	−0.052
nuclear–e^- attractn	−5770.355	−5770.152	+0.203
electron repulsns	+1470.884	+1470.790	−0.094
total energy	−1773.393	−1773.380	+0.013

[a] All energies in atomic units.

A population analysis of the bent 130° structures reveals a similar negatively charged nitrosyl when bent in both the CO and CN planes, as one would expect for an {FeNO}^{8} system. If one views the respective bending planes of these two structures (**2** and **3**), a simple electrostatic rationale for

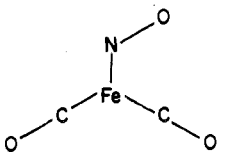

2

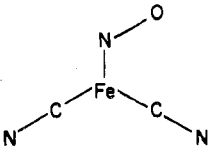

3

the preferred geometry presents itself. The nuclear charge difference between the cyanide nitrogen and the carbonyl oxygen is sufficient to cause the nuclear–electron attraction to be larger for the CO plane conformer. Thus, the negatively charged nitrosyl is stabilized to a greater extent in the CO plane structure (**2**) by the oxygen nuclear charge than in the CN plane structure (**3**) by the nitrogen nuclear charge. Although, at first glance, this explanation appears to differ from the explanation in terms of the π-acceptor ability of the ligands,[6] it is totally consistent with these previous explanations. For a diatomic ligand AB (M–AB) increasing the nuclear charge on B(CN^- vs. CO, N_2 vs. NO^+) or increasing the nuclear charge on A(CO vs. NO^+) leads to a stronger π acceptor in each case. Thus, both explanations of the preferred plane of bending are closely related.

Recently, Noell and Morokuma[32] have reported ab initio RHF calculations on $[Co(NH_3)_5NO]^{2+}$ with the nitrosyl eclipsing the Co–NH_3 bond and with the nitrosyl staggered between two Co–NH_3 bonds. Their results show that the staggered geometry is 6 kcal/mol higher in energy and that this energy difference is due to the electrostatic term in their energy decomposition scheme, in essential agreement with our results. Because of the relatively small energy difference, there are a number of cases where packing forces, steric bulk of the ligands, or more subtle electronic effects cause the nitrosyl to adopt a staggered or partially staggered geometry.[33]

Acknowledgment. The authors thank the National Science Foundation (Grant No. CHE 77-07825) for support of this work.

Registry No. $[Fe(CN)_4NO]^-$, 60706-14-1; $[Fe(CN)_4NO]^{2-}$, 51232-23-6; $[Fe(CN)_4NO]^{3-}$, 58904-86-2; $[Fe(CO)_2(CN)_2NO]^-$, 73246-59-0.

(32) Noell, J. O.; Morokuma, K. *Inorg. Chem.* **1979**, *18*, 2774.
(33) (a) Haller, K. J.; Enemark, J. H. *Acta Crystallogr., Sect. B* **1978**, *34*, 102. (b) Kelly, B. A.; Welch, A. J.; Woodward, P. *J. Chem. Soc., Dalton Trans.* **1977**, 2237. (c) Karlin, K. D.; Rabinowitz, H. N.; Lewis, D. L.; Lippard, S. J. *Inorg. Chem.* **1977**, *16*, 3262. (d) English, R. B.; Nassimbeni, L. R.; Haines, R. J. *Acta Crystallogr., Sect. B* **1976**, *32*, 3299.